Kinetic Analysis of Phospholipid Exchange between Phosphatidylcholine/Taurocholate Mixed Micelles: Effect of the Acyl Chain Moiety of the Micellar Phosphatidylcholine†

Doug A. Fullington and J. Wylie Nichols*

Department of Physiology, Emory University School of Medicine, Atlanta, Georgia 30322

Received June 29, 1993; Revised Manuscript Received September 16, 1993®

ABSTRACT: A fluorescent assay based on concentration-dependent self-quenching of the fluorescent phospholipid *N*-(7-nitrobenz-2-oxa-1,3-diazol-4-yl)phosphatidylethanolamine was used to measure the rate of phospholipid exchange between taurocholate/phosphatidylcholine mixed micelles. Two NBD-labeled phosphatidylethanolamine probes (dilauryl and dimyrisotyl) were tested in taurocholate/phosphatidylcholine mixed micelles prepared from phosphatidylcholine molecules varying in saturated chain length from 12 to 18. All combinations of probes and micellar phosphatidylcholines gave kinetic results that were best described by a transfer model in which phospholipids exchange predominantly through the water phase at low micellar concentrations and through transient micelle fusions at higher concentrations. Increasing the chain length of the micellar-saturated diacylphosphatidylcholine from 12 to 18 carbons resulted in a decrease in the overall rate of exchange by a factor of 127 for NBD-labeled dilaurylphosphatidylethanolamine and a factor of 2490 for NBD-labeled dipalmitoylphosphatidylethanolamine. The reduction in the overall rate resulted from decreases in both mechanisms of transfer. These results argue that the hydrophobicity of the lipophilic core of bile salt/phospholipid mixed micelles is the predominant determinant of the rate of formation of transfer-competent, transient micelle fusions and a major determinant of the rate of micelle to water phospholipid dissociation.

Mixed micelles have been shown to coexist with simple bile salt micelles and bilayer vesicles composed of bile salts, phospholipids, and cholesterol in mixtures of model bile. The relative distribution of these aggregates depends upon both the relative and total concentrations of the lipid components (Carey, 1985; Cabral and Small, 1989). Determination of the distribution of these aggregates is important to understanding the physiological function of bile since the aggregate structures differ dramatically in their ability to solubilize cholesterol (Donovan and Carey, 1990) and facilitate lipid absorption (Staggers et al., 1990). The development of equilibrium phase diagrams for these model biles has allowed the prediction of the aggregate structure distribution when the composition of the model bile is known. However, the enterohepatic circulation is a dynamic system and the transition between aggregates occurs in response to both gradual and abrupt changes in the relative concentrations of the lipid components. For example, the relative lipid concentrations in hepatic bile depend on the independent and variable rates of phospholipid, bile salt, and cholesterol secretion. Water reabsorption from the gall bladder lumen results in a gradual increase in lipid concentration, and release of bile into the small intestine following gall bladder contraction results in a rapid dilution. The rates at which structural rearrangements occur in response to these changes must be taken into account in developing a dynamic model for the functions of bile in the enterohepatic circulation.

In this paper, we have measured the rates of phospholipid transfer between bile salt/phospholipid mixed micelles as a function of acyl chain length and unsaturation of the mixed micelle phospholipid molecules. These rate measurements were combined with a kinetic analysis to determine the mechanism of phospholipid transfer and yielded important fundamental insight into this basis step required for the aforementioned aggregate transitions. Phospholipids, labeled with the fluorescent probe NBD[1] (7-nitrobenz-2-oxa-1,3-diazol-4-yl), were used to measure the rates of phospholipid exchange between mixed micelles. We have used this technique previously to conclude that, at relatively high concentrations of mixed micelles (>1 mM phospholipid), transfer occurs predominantly as a result of micelle collisions, whereas, at low mixed micelle concentrations (<1 mM phospholipid), the transfer occurs through the water phase (Nichols, 1988; Fullington et al., 1990). The transfer through the water phase is facilitated by the interaction of monomeric phospholipid with small multimers of bile salts (Shoemaker and Nichols, 1990, 1992). The rate of exchange via both pathways is highly dependent on the bile salt structure and is roughly correlated with their hydrophobicity (Fullington et al., 1990). Herein, we demonstrate that decreasing the acyl chain length of the phospholipids in the mixed micelle dramatically increases the rate of NBD-labeled phospholipid transfer by both pathways. The introduction of a cis double bond into the acyl chain has a similar effect.

† This study was supported by U.S. Public Health Service Grant DK 40641.

* To whom correspondence should be addressed.

® Abstract published in *Advance ACS Abstracts,* November 1, 1993.

[1] Abbreviations: NBD, 7-nitrobenz-2-oxa-1,3-diazol-4-yl; *N*-NBD-PE, *N*-(NBD)diacylphosphatidylethanolamine; *N*-NBD-DLPE, *N*-(NBD)dilaurylphosphatidylethanolamine; *N*-NBD-DMPE, *N*-(NBD)dimyristoylphosphatidylethanolamine; PC, diacylphosphatidylcholine; DLPC, dilaurylphosphatidylcholine; DMPC, dimyristoylphosphatidylcholine; DPPC, dipalmitoylphosphatidylcholine; DSPC, disteroylphosphatidylcholine; DOPC, dioleoylphosphatidylcholine; DSPA, disteroylphosphatidic acid; TC, taurocholate; HBS, HEPES-buffered saline, 0.9% NaCl in 10 mM; HEPES, 4-(2-hydroxyethyl)-1-piperazineethanesulfonic acid, pH 7.4.

0006-2960/93/0432-12678$04.00/0

EXPERIMENTAL PROCEDURES

Materials and Routine Procedures. DLPC, DMPC, DPPC, DSPC, DSPA, POPC, dilaurylphosphatidylethanolamine, and *N*-NBD-DMPE were purchased from Avanti Polar Lipids, Inc. *N*-NBD-DLPE was synthesized by reacting NBD-chloride with dilaurylphosphatidylethanolamine (Struck et al., 1981) and was purified by silica gel thin-layer chromatography. All lipids resulted in only one spot by TLC when 50–100 μg of PC's and 10–20 μg of N-NBD-PE's were spotted onto TLC plates, run in acidic, neutral, and basic solvent systems, and then visualized using sulfuric acid charring or ultraviolet light, respectively. A 200-μg sample of taurocholate (Sigma Chemical Co.) produced a single spot on silica gel thin-layer chromatography plates run in a 65:25:2:4 chloroform:methanol:acetic acid:water mixture and developed by sulfuric acid charring. NaCl (J. T. Baker), sodium azide (Sigma Chemical Co.), and HEPES (United States Biochemical) were ACS or reagent grade. Taurocholate (TC) solution concentrations were determined by weight, and phospholipid concentrations were determined by a lipid phosphorous assay (Ames & Dubin, 1960). Lipids were stored in chloroform at −20 °C, and taurocholate was stored as a powder under vacuum at room temperature. TC solutions in methanol and HBS were prepared from powder prior to each use.

Mixed Micelle and Vesicle Preparation. Mixed PC/TC micelles were prepared by drying equimolar amounts of a chloroform solution of phosphatidylcholine and a methanol solution of taurocholate under a stream of nitrogen in order to spread a thin lipid film on the bottom of a round-bottom flask. The film was desiccated under vacuum at least 6 h before the addition of taurocholate in HBS to achieve the desired final concentrations of 10:20 mM PC/TC for acceptor micelles and 2:8:20 mM *N*-NBD-PE/PC/TC for donor micelles. The resulting micelle solutions were dialyzed overnight at room temperature in Spectra/Por 3 dialysis bags (molecular weight cutoff 3500) against 4 mM taurocholate in HBS. Small unilamellar vesicles were prepared by bath sonication of a 1 mM solution of 95:5 mol % DSPC/DSPA in HBS. Large multilamellar vesicles were prepared by drying a chloroform solution of POPC with a stream of nitrogen. Following overnight vacuum desiccation, the POPC was resuspended in HBS with a vortex mixer.

Fluorescence and Light-Scattering Measurements. Light-scattering and slow fluorescent transients ($t_{1/2} > 2$ s) were measured using a Perkin-Elmer MPF-44E fluorescence spectrophotometer [see Nichols (1988)]. Analog output was digitized and stored on an IBM XT computer for subsequent kinetic analysis. Cuvette solutions were continuously stirred by a magnetic stirrer, and a constant temperature was maintained with a circulating water bath. Inner filtering was minimized by using *N*-NBD-PE concentrations which resulted in less than 0.2 absorbance at the maximum excitation wavelength. Fast fluorescence transients ($t_{1/2} < 2$ s) were measured using an SLM 8000C spectrofluorometer equipped with an SLM stopped-flow device. A circulating water bath maintained a constant temperature, and the digital output was stored on an IBM AT-compatible computer.

Measurement of N-NBD-PE Transfer between Micelles. The technique for using concentration-dependent self-quenching of the fluorescent probe *N*-NBD-PE to measure its transfer between donor and acceptor micelles has been described previously (Nichols, 1988; Fullington et al., 1990). Briefly, donor micelles were prepared containing 20 mol % *N*-NBD-PE, which resulted in about a 50% reduction in the fluorescence signal due to self-quenching. The donor micelles were either injected into a cuvette containing acceptor micelles (without probe) or mixed with acceptor micelles with a stopped-flow mixing device. Prior dialysis of both the donor and acceptor micelles against 4 mM TC established the concentration of water-soluble, non-micelle-associated TC at this concentration. Thus, all experiments were performed by diluting the donor and acceptor micelles into 4 mM TC to avoid altering the micellar PC to TC ratio which affects the micellar size and extent of fluorescence quenching (Mazer et al., 1980; Nichols & Ozarowski, 1990). Therefore, the increase in fluorescence observed following mixing was due to the loss of self-quenching as the *N*-NBD-PE equilibrated into the unlabeled acceptor micelles. All of the fluorescence traces obtained by this procedure could be accurately fit by a single-exponential function, and additional exponential terms did not improve the goodness of fit. A nonlinear least-squares fitting program written by Bill Goolsby in the Department of Anatomy and Cell Biology, Emory University, and based on the Marquardt algorithm (Marquardt, 1963) was used to obtain the parameters giving the best fit to the experimental data.

Kinetic Analysis of Fluorescence Data. Since the initial rate of fluorescence increase can be directly correlated to the rate at which *N*-NBD-PE transfers between micelles [see Nichols (1988) and Fullington et al. (1990)], the apparent rate constant (k_{app}; see Figure 1) and the amplitude (ΔF_{eq}) obtained from the exponential fits were used to obtain the initial rate of fluorescence increase ($\Delta F_{t=0}/\Delta t$) since by definition for an exponential function $\Delta F_{t=0}/\Delta t = k_{app}(\Delta F_{eq})$. Division of the initial rate by the maximum fluorescence change (ΔF_{max}) gives the initial fractional rate of fluorescence change. The maximum fluorescence change is the amplitude obtained at equilibrium after the donors are diluted into excess acceptor micelles, resulting in a maximum fluorescence signal. In all experiments, the donor micelle concentrations were 0.033 mM PC and the maximum fluorescence signal at equilibrium was reached at least by a concentration of 5 mM acceptor micelles PC. Using the initial fractional rate of fluorescence increase, the initial rate of *N*-NBD-PE transfer from donors to acceptors can be calculated by the following equation derived in Fullington et al. (1990):

$$R = \frac{(\Delta[D]_2)_{t=0}}{[D]_T \Delta t} = \frac{1 + \Delta F_{max}/F_0}{2 + \Delta F_{max}/F_0} \frac{\Delta F_{t=0}}{\Delta F_{max} \Delta t} \quad (1)$$

R is the initial rate of *N*-NBD-PE transfer from donors to acceptors, expressed as the fraction of total transfer per second, $(\Delta[D]_2)_{t=0}$ is the bulk solution concentration of *N*-NBD-PE transferred to acceptor micelles during the initial rate period (Δt), $[D]_T$ is the total bulk solution concentration of *N*-NBD-PE, and F_0 is the fluorescence yield at $t = 0$.

Kinetic Models for N-NBD-PE Transfer between Micelles. *N*-NBD-PE transfer between micelles has been shown to occur by two mechanisms—diffusion through the aqueous phase and transfer during transient collisions between two or three micelles (Nichols, 1988; Fullington et al., 1990). Given the special experimental case in which the donor and acceptor micelles are identical, the initial rates of transfer for each mechanism are predicted by the following equations:

$$\text{aqueous diffusion:} \quad R = k_{dis}[L]_2/([L]_1 + [L]_2) \quad (2)$$

$$\text{bimolecular collision:} \quad R = k_{bi}[L]_2 \quad (3)$$

$$\text{termolecular collision:} \quad R = k_{ter}([L]_2)^2 \quad (4)$$

$[L]_1$ and $[L]_2$ are the bulk solution concentrations of PC in the donor and acceptor micelles, respectively; k_{dis}, k_{bi}, and k_{ter} are the aqueous dissociation, bimolecular collision, and

termolecular collision rate constants, respectively. The mechanism or combination of mechanisms that best describe the initial rate data was obtained by fitting plots of initial rate (R) versus acceptor micelle PC concentration to all possible combinations of the above three models. Curve fitting was performed with the nonlinear-least-squares program described above, and the combination of equations which gave the best fit was determined by using the F_x test to test whether addition of an additional equation increased the goodness of the curve fit to the data [see p 200 in Bevington (1969)]. This statistic follows the F distribution with one degree of freedom and can be used to test the null hypothesis that the coefficient of the added term is equal to zero (i.e., the new term does not improve the goodness of fit).

High-Performance Liquid Chromatography. High-performance liquid chromatography was carried out using a Rainin Rabbit-HP pump with 5-mL pump heads as described previously (Nichols & Ozarowski, 1990). Sample separations were achieved with a TSK 5000 PW column preceded by an in-line 5-μm filter. Micelles, vesicles, and proteins were detected by measuring optical density changes at wavelength 280 nm with a Spectromonitor D variable-wavelength detector (LDC/Milton Roy) and recording the signal and elution volumes with a Shimadzu Chromatopac C-R3A. The column was equilibrated with 150 mL of the appropriate buffer [HBS for column calibration with globular proteins (1 mg/mL) and vesicles (1 mM 95:5 mol % DSPC/DSPA), HBS without sodium azide for the azide determination of total column volume, and the 4 mM TC in HBS postdialysis buffer for mixed micelles]. Aliquots of 50–100 μL were injected into the sample loop and run at a flow rate of 1 mL/min with a pressure less than 12 kg/cm^2 ($\sim$170 psi). Total column volume was determined from the elution volume of sodium azide (V_t = 10.18 mL), and excluded volume was determined from the elution volume of large multilamellar vesicles (V_o = 4.88). Elution volumes (V_e) of samples were transformed to K_d values, where $K_d = (V_e - V_o)/(V_t - V_o)$. A standard curve for sizing mixed PC/TC micelles was prepared using globular proteins and phospholipid vesicles of known size as previously described (Nichols & Ozarowski, 1990). The column was calibrated with these standards according to the equation of Ackers (1967) (Nozaki et al., 1976):

$$r = a_o + b_o \operatorname{erf}^{-1}(1 - K_d) \quad (5)$$

where r is the hydrodynamic radius, and a_o and b_o are constants describing the size distribution of the gel pores. $\operatorname{erf}^{-1}(x)$ is the inverse error function of the Gaussian distribution function when $\operatorname{erf}(x) = 1 - (2/\pi^{1/2})\exp(-x^2)\,dx$. Values for $\operatorname{erf}^{-1}(1 - K_d)$ were obtained from a table of error functions (NBS Applied Mathematics Series 41).

RESULTS

Measurement of N-NBD-PE Transfer between Mixed Micelles. An illustration of the method used to measure the transfer of N-NBD-PE between PC/TC micelles is shown in Figure 1. At B a small aliquot of donor micelles containing self-quenching concentrations of N-NBD-DMPE was injected into a cuvette containing DMPC/TC acceptor micelles added at A. Different fluorescent traces were obtained depending on the concentration of acceptor micelles in the cuvette. When no acceptor micelle PC was added to the cuvette, and the donor micelles were injected into 4 mM TC, a constant level of fluorescence was observed following the initial rapid increase. The initial rapid increase (F_0) reflects the unquenched fluorescence in the donor micelles. The absence of

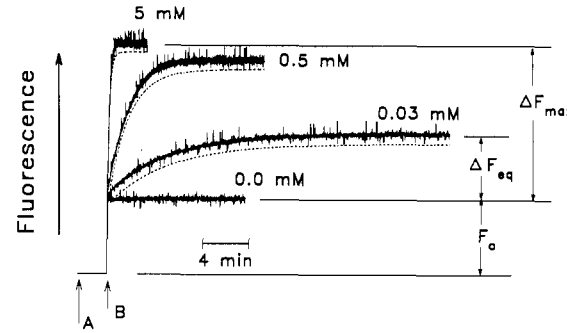

FIGURE 1: Fluorescence traces of N-NBD-DMPE transfer between DMPC/TC mixed micelles. At A, fluorescence was recorded (ex 475 nm; slit width 4 nm; em 530 nm, slit width 4 nm) from a cuvette containing different concentrations of acceptor mixed micelles (DMPC/TC; 10/20 mM) added to 4 mM TC in HBS in a final volume of 1.5 mL. At B, 5 μL of donor micelles (N-NBD-DMPE/DMPC/TC; 2/8/20 mM) was injected into the cuvette and the increase in fluorescence was recorded (solid lines). Final concentration of donor micelles was 0.033 mM phospholipid (N-NBD-DMPE + DMPC). Final concentrations of acceptor micelle DMPC are labeled above the corresponding trace. Temperature = 25 °C. The fluorescence traces were fit to a single-exponential function with an offset, and the best fit parameters were used to generate theoretical curves (dotted lines) which were plotted below the fluorescence traces to allow comparison. The parameters ΔF_{eq}, F_0, and the apparent first-order rate constants (k_{app}) were obtained from the best fits to the data. ΔF_{max} is defined as the maximum ΔF_{eq} obtained following equilibration into excess acceptor micelles.

a transient change in fluorescence indicates that the donor micelles are in equilibrium with 4 mM TC. When donor micelles are injected into the cuvette containing acceptor mixed micelles, the observed increase in fluorescence reflects the transfer and dilution of N-NBD-DMPE from self-quenching concentrations in the donor micelles to the nonquenching acceptor micelles. For each trace, the best values for k_{app}, ΔF_{eq}, and F_0 were obtained from a fit to a single-exponential function. The average of ΔF_{eq} for the three highest acceptor concentrations (3, 4, and 5 mM PC) was used as the value for ΔF_{max}. These parameters were used to calculate the initial fractional rate of N-NBD-PE transfer (R) at each acceptor concentration for eq 1.

Effect of Phospholipid Acyl Chain Length on N-NBD-DMPE Transfer. Plots of the initial rates of N-NBD-DMPE transfer between PC/TC mixed micelles as a function of the acceptor micelle PC concentration for a series of saturated diacyl PC's are presented in Figure 2. For each PC, the initial rate of transfer increased as the concentration of acceptor micelles was increased. The data for each PC were fitted to the simplest combination of kinetic models (aqueous diffusion and bimolecular or termolecular collision; eqs 2–4) that described the data. This analysis indicated that for each of the four PC molecules a term based on the aqueous diffusion model was required to fit the data at low acceptor micelle concentrations and a term based on the bimolecular and/or termolecular collision model was required to describe the data at higher acceptor concentrations.

Regardless of the mechanisms involved in transfer, the half-time for the intermicellar transfer of N-NBD-DMPE decreased dramatically as the acyl chain length of the micellar PC was increased (Table I). For example, N-NBD-DMPE transferred 2400 times faster between micelles comprising DLPC than between those comprising DSPC. In Figure 4, the bimolecular and termolecular rate constants are combined to give a single apparent rate constant for collision-dependent transfer (k_{coll}) at 5 mM acceptor micelle PC. These results illustrate that both the rate of transfer through the water

Table I: Rate Constants for the Intermicellar Transfer of *N*-NBD-DMPE[a]

phosphatidylcholine	acyl chain	$t_{1/2}$ (s)[b]	k_{dis} ($s^{-1} \times 10^4$)[c]	k_{bi} ($M^{-1}\cdot s^{-1}$)[d]	k_{ter} ($M^{-2}\cdot s^{-1}$)[e]
DLPC	12:0	0.84 ± 0.045	184 ± 22	162 ± 1.9	*f*
DMPC	14:0	11.6–11.8	11.2 ± 2.3	8.92 ± 0.41	514 ± 76
DPPC	16:0	762 ± 217	1.81 ± 0.11	0.053 ± 0.004	18.5 ± 0.8
DSPC	18:0	2087 ± 388	1.47 ± 0.27	*f*	7.4 ± 0.4
DOPC[g]	18:1	9.3	34 ± 5.1	7.8 ± 0.5	1300 ± 8.5

[a] Experiments were performed at 25 °C. Rate constants were calculated using the kinetic rate equations (2)–(4) as described under Experimental Procedures. [b] $t_{1/2}$ ± sd was calculated from the apparent rate constant obtained at 5 mM acceptor PC. [c] Dissociation rate constant. [d] Bimolecular rate constant. [e] Termolecular rate constant. Rate constants are presented ± the standard error of the fit parameters calculated according to Bevington (1969). [f] Inclusion of this term did not significantly increase the goodness of fit. [g] Data for DOPC are reproduced from Nichols (1988).

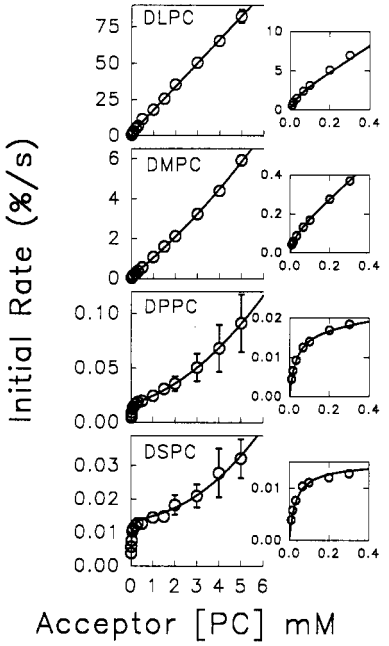

FIGURE 2: Initial rates of *N*-NBD-DMPE transfer between PC/TC mixed micelles as a function of the acceptor micelle PC concentration for a series of saturated diacyl PC's. Plots on the left illustrate the full range of acceptor micelle PC concentrations. The smaller plots on the right show expansion of the data at low concentrations. Transfer measurements were made as illustrated in Figure 1 and the initial rates calculated as described under Experimental Procedures. Open circles and error bars represent the average of three experiments plus or minus the standard deviations. Error bars falling within the symbol were omitted. The solid lines were generated from the best fits of the data as described under Experimental Procedures. Rate constants obtained from the best fits of the data are presented in Table I.

(k_{dis}) and the rate of transfer during transient micelle collisions (k_{coll}) are decreased as the acyl chain length is increased. For comparison, the rate constants obtained for intermicellar transfer between micelles containing DOPC obtained in previous work (Nichols, 1988) are included in Table I and Figure 4. These data demonstrate that the rate of intermicellar transfer of *N*-DMPE by both the aqueous diffusion and the collision-dependent pathways is faster for monosaturated PC's of the same chain length.

Effect of Acyl Chain Length on N-NBD-DLPE Transfer. In order to determine more accurately the effect of the acyl chain length of the micellar PC on the aqueous diffusion pathway at low concentrations, analogous experiments were performed using the shorter acyl chain probe *N*-NBD-DLPE. Because of its shorter acyl chains, this probe dissociates from micelles more readily than does *N*-NBD-DMPE such that the dissociation rate constant can be measured more accurately. These data are presented in Figure 3, and rate constants obtained from the curve fits are presented in Table II and Figure 4. These results are similar to those obtained for

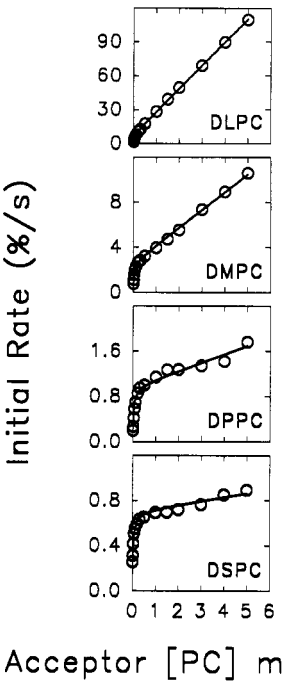

FIGURE 3: Initial rates of *N*-NBD-DLPE transfer between PC/TC mixed micelles as a function of the acceptor micelle PC concentration for a series of saturated diacyl PC's. Transfer measurements were made as illustrated in Figure 1 and the initial rates calculated as described under Experimental Procedures. Open circles are the measured initial rates. Solid lines were generated from the best fits of the data as described under Experimental Procedures. Rate constants obtained from the best fits of the data are presented in Table II.

Table II: Rate Constants for the Intermicellar Transfer of *N*-NBD-DLPE[a]

phospha-tidylcholine	acyl chain	$t_{1/2}$ (s)[b]	k_{dis} ($s^{-1} \times 10^2$)[c]	k_{bi} ($M^{-1}\cdot s^{-1}$)[d]	k_{ter} ($M^{-2}\cdot s^{-1}$)[e]
DLPC	12:0	0.63	7.9 ± 0.3	205 ± 1.2	*f*
DMPC	14:0	6.60	2.6 ± 0.2	15.7 ± 0.4	*f*
DPPC	16:0	40.9	0.96 ± 0.05	1.46 ± 0.2	*f*
DSPC	18:0	79.9	0.71 ± 0.03	0.32 ± 0.12	*f*
DOPC[g]	18:1	5.6	3.3 ± 0.1	12.0 ± 1.0	1200 ± 94

[a] Experiments were performed at 25 °C. Rate constants were calculated using the kinetic rate equations (2)–(4) as described under Experimental Procedures. [b] $t_{1/2}$ was calculated from the apparent rate constant obtained at 5 mM acceptor PC. [c] Dissociation rate constant. [d] Bimolecular rate constant. [e] Termolecular rate constant. [f] Inclusion of this term did not significantly increase the goodness of fit. [g] Data for DOPC are reproduced from Nichols (1988).

N-NBD-DMPE in that the rate of *N*-NBD-DLPE intermicellar transfer via both the aqueous diffusion and collision-dependent pathways increases with decreasing acyl chain length and unsaturation.

Effect of Acyl Chain Length on Micellar Size. To determine if PC acyl chain length affected the micelle size, the average

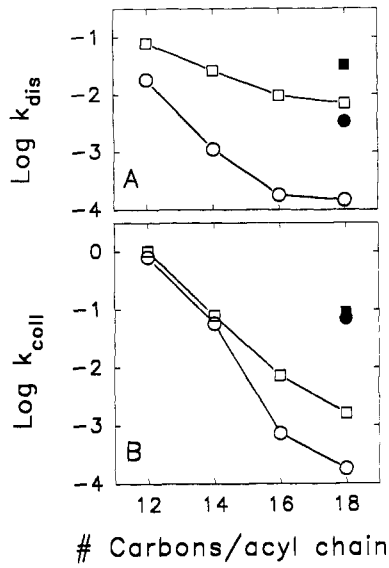

FIGURE 4: Log plots of dissociation (k_{dis}) and collision (k_{coll}) rate constants as a function of PC acyl chain length. The collision-dependent rate constant (k_{coll}) is defined as the apparent first-order rate constant for transfer occurring by both the bimolecular and termolecular collision pathways at 5 mM acceptor PC concentration: $k_{coll} = k_{bi}(5\text{ mM}) + k_{ter}(5\text{ mM})^2$. Values for k_{dis}, k_{bi}, and k_{ter} are listed in Tables I and II. Circles and squares represent transfer of *N*-NBD-DMPE and *N*-NBD-DLPE, respectively. Open symbols refer to transfer between PC/TC mixed micelles comprising saturated diacyl PC (DLPC, DMPC, DPPC, and DSPC), and closed symbols refer to transfer between mixed micelles comprising monounsaturated diacyl PC (DOPC).

hydrodynamic radii of the various PC/TC micelles were measured by size exclusion chromatography as described under Experimental Procedures. The results (Table III) show a slight trend toward larger micelles as the acyl chain length is increased, but the measured hydrodynamic radii do not correlate with the rate constants plotted in Figure 4. Furthermore, the maximum 2-fold difference in the hydrodynamic radii measured between DLPC and DPPC cannot account for the hundred- to thousand-fold changes observed for the transfer rates. Thus, although some of the differences in transfer rates may be the result of acyl chain length of the micellar size, the majority of these differences must be the result of variations in other physical properties of the micelles.

DISCUSSION

In this paper, we have used two different NBD-labeled diacyl phospholipids to investigate the effect of micellar phospholipid chain length and unsaturation on the rate and mechanisms of phospholipid exchange between TC/PC mixed micelles. The data are consistent with a kinetic model based on the assumption that, at low micelle concentrations, the predominant mode of phospholipid transfer results from their dissociation from the donor micelle into the water phase followed by insertion into an acceptor micelle and, at higher micelle concentrations, phospholipid transfer occurs during transient collisions or fusions of donor and acceptor micelles. The fit of the data to this model is consistent with previous results from this laboratory. The model accurately predicts the kinetic behavior of mixed micelles containing *N*-NBD-PE of different chain lengths (Nichols, 1988) and a wide range of bile salts (Fullington et al., 1990). The consistent agreement of these results argues that this kinetic model for intermicellar phospholipid exchange is generally applicable to a wide range of bile salt/phospholipid mixed micelle compositions.

Table III: Sizing of Micelles by HPLC[a]

particle	V_e (mL)[b]	radius (Å)[c]
	Standards	
BSA	8.52 ± 0.01 (3)	30.6[d]
apoferritin	7.68 ± 0.14 (4)	61.6[e]
DSPC/DSPA vesicles	5.14 ± 0.09 (7)	163[f]
	Mixed Micelles	
DLPC/TC	8.64 ± 0.11 (3)	34.1 ● 2.5
DMPC/TC	8.42 ± 0.08 (4)	37.2 ± 2.9
DPPC/TC	7.40 ± 0.09 (3)	62.1 ● 1.6
DSPC/TC	8.06 ± 0.01 (3)	46.2 ● <0.1

[a] Particle sizes were determined according to the method described in Experimental Procedures using the standards listed. [b] V_e is the elution volume. [c] Hydrodynamic radius for micelles was obtained from the calibration line for proteins and vesicles of known size. [d] Radius determined by X-ray diffraction (Kumosinski & Pesson, 1985). [e] Radius determined from the hydrodynamic relationship of molecular weight to molecular volume (Himmel & Squire, 1981). [f] Radius determined by quasi-elastic light scattering by the method of Menger et al. (1989).

Our data demonstrated that the rates of transfer by both mechanisms decreased as the acyl chain length of the saturated diacyl PC in the micelles was increased. Insertion of a single double bond into each acyl chain resulted in an increase in the rate constants for both mechanisms that is roughly equivalent to decreasing the length of both acyl chains by two carbons. Since the only variable in these experiments is the acyl chain composition, the data argue that the rates of phospholipid dissociation into the water phase as well as the rates of transient micellar collision depend on the hydrophobicity of the micelle interior.

However, changes in the micellar PC acyl chain length could also affect the size of the micelles as well as the phase state of the micellar PC molecules. Measurements of the micelle size (Table III) indicated small increases in the hydrodynamic radii with increasing acyl chain length, but the large increases in the rate constant for aqueous dissociation and the rate constant for collision-dependent transfer do not correlate with the small changes in size. Thus, we concluded that micellar size was not the primary determinant of the observed decreases in transfer rates with increasing acyl chain length.

Differential scanning calorimetry scans of TC/DPPC mixed micelles with a high TC to DPPC ratio (as used in this study) indicate a broad structureless peak representing a single phase transition that occurs near 5 °C (Spink et al., 1991). One would predict from these measurements that, at the temperature of our rate measurements, 25 °C, the mixed micelles prepared from the five different PC molecules would all be above this phase transition temperature and exist in the same fluid-phase state. Thus, changes in phase state as a function of PC acyl chain length can be excluded from the interpretation of the rate data.

Acyl Chain Dependence of the Micelle to Water Dissociation Rate. As the acyl chain length of the micellar PC was increased from 12 to 18, the dissociation rate constant decreased by a factor of 11 for *N*-NBD-DLPE and a factor of 124 for *N*-NBD-DMPE (Table II; Figure 4). Thus, the acyl chain length of the micellar PC has a greater effect on dissociation of the longer chained *N*-NBD-DMPE than on that of *N*-NBD-DLPE but has a significant effect on both. These observations indicate that the free energy of both of the probes residing in the micelle is reduced in micelles comprising PC molecules with longer acyl chains. Reduction in the free energy of the probe molecules residing in the micelles increases the activation energy and therefore reduces the rate for their dissociation

into the water (Nichols, 1985). The free energy of *N*-NBD-PE molecules in the micelles would be reduced if the size of the hydrophobic micellar core into which water is unable to penetrate is larger for micelles comprising longer chain PC molecules. Alternatively, increased chain length might also increase the extent of van der Waals interactions between the micellar PC acyl chains and those of the probe molecules. One or both of these possibilities could explain the observed dependence of the micelle to water dissociation rate on micellar PC acyl chain length. Addition of a double bond to the micellar PC would be expected to have effects on the extent of water penetration and van der Waals interactions similar to those of decreasing the acyl chain length. The effect of micellar PC chain length begins to saturate for acyl chains longer than 16 carbons, suggesting that micelles composed of 16-carbon acyl chains approach the maximum hydrophobic, low free energy environment for the two *N*-NBD-PE probes.

Acyl Chain Dependence of Collision-Dependent Transfer. Figure 4 illustrates that the apparent first-order rate constant for collision-dependent transfer (k_{coll}) is almost a linear log function of the number of carbons in the micellar PC's. Increasing the acyl chain length from 12 to 18 results in over a 4300-fold reduction in the collision-dependent rate for *N*-NBD-DMPE and a 780-fold reduction for *N*-NBD-DLPE. To aid in the interpretation of these results, the bimolecular rate constant can be expressed as the product of several parameters and rate constants that describe the individual events involved in the successful collision and transfer of phospholipids (Nichols, 1988):

$$k_{bi} = \frac{k_c \alpha \beta_1}{n_L^2}$$

where k_c is the diffusion-limited collision rate constant, α is the fraction of phospholipid molecules exchanged during the lifetime of a transient fusion complex, β_1 is the fraction of micelle collisions that result in a transient fusion complex capable of exchanging phospholipids, and n_L is the number of phospholipid molecules per micelle. Although the average size of the micelles is increased slightly as the acyl chain length of the micellar PC molecules is increased, the maximum size change is a factor of 2. This would increase the value of n_L by the same factor and the value of k_{bi} by a factor of 4. These are relatively small changes relative to the large differences in collision-dependent rates measured. Thus, although increases in micellar size may reduce the rate of collision-dependent transfer by a factor of 4, the predominant effect is on the hydrophobicity of the micelle interior. Nor would the small changes in micellar size be predicted to significantly reduce the diffusion-limited collision frequency of the micelles, k_c. Since these micelles are above the phase transition temperature, it is reasonable to assume that the fraction of the micellar phospholipid that exchanges during the formation of a transient fusion complex, α, is constant. Thus, the primary effect of the acyl chain length is on the rate of formation of transfer-competent transient fusion complexes.

The dependence on the rate of transient fusion complex formation on acyl chain length and saturation argues that the activation energy for fusion includes the energy required to separate and mix the acyl chains in the micelle interior in addition to the energy of dehydration involved in bringing the two micelles into close apposition. The relative contributions of these two energy barriers can be estimated by calculating the activation energies for formation of the fusion complex from the Eyring activated complex theory. The *y* intercept of a plot of these activation energies as a function of acyl chain length predicts the activation energy for fusion complex formation between theoretical micelles which have no hydrophobic micellar core but which have surface and size properties identical to those of the experimental micelles. The data in Table II for the bimolecular collision contants, k_{bi}, must first be converted to represent micelle concentrations as opposed to PC concentrations. This is accomplished by multiplying k_{bi} times n_L^2. Recent data indicate that bile salt/PC mixed micelles in the concentration range of the micelles used in these experiments are in the shape of elongated rods (Ulmius et al., 1982; Nichols & Ozarowski, 1990; Hjelm et al., 1992). There are approximately 94 phospholipid molecules in a rod-shaped micelle with a hydrodynamic radius of 41 Å (Nichols & Ozarowski, 1990). After conversion of k_{bi} to micelle concentration units, the calculated activation energies for formation of transient fusion complexes are 8.9, 10.4, 11.8, and 12.7 kcal/mol for micelles with diacyl PC's of 12; 14; 16; and 18-carbon acyl chain lengths, respectively. A linear regression fit of this data gives a *y* intercept of 1.3 kcal/mol and a slope of 0.64 kcal/(mol·carbon), with a linear correlation coefficient of 0.994. From this analysis one can conclude that the majority of the activation barrier arises from the energy required to fuse the hydrophobic cores as opposed to the energy required to bring the surfaces close together.

Physiological Significance. The results discussed above indicate that the molecular species of phosphatidylcholine components of mixed micelles have a profound influence on the rates of distribution and exchange of the micellar components. Fewer double bonds and/or longer acyl chain lengths significantly retard the exchange of micellar components necessary for mixed micelle formation in the liver and gallbladder as well as lipid digestion in the intestine. In studies of model bile, lecithins with shorter, more unsaturated fatty acids were shown to partition preferentially into mixed micelles in equilibrium with cholesterol-saturated vesicles (Cohen & Carey, 1991). Furthermore, these less hydrophobic lecithins solubilized more cholesterol in both the micelles and vesicles. This increased capacity to solubilize cholesterol in combination with the faster exchange rates for the less hydrophobic lecithins suggests that modulation of the molecular species of lecithin in the bile may provide a mechanism to increase the solubility of cholesterol in bile and to increase the dynamic exchange of lipid components necessary for rapid aggregate transitions throughout the biliary tree and lipid absorption in the intestine. Given that the molecular species of lecithin in the bile and the intestine can be influenced by exogenously administered bile salts (Booker et al., 1990a, 1990b) as well as diet (Salvioli et al., 1985) and disease (Kajiyama et al., 1980; Ahlberg et al., 1981; Cantafora et al., 1981; Hay et al., 1993), these results indicate that knowledge of the regulation of the molecular species of biliary PC is essential to a thorough understanding of normal bile function and related pathology.

REFERENCES

Ackers, G. K. (1967) *J. Biol. Chem. 242*, 3237–3238.
Ahlberg, J., Curstedt, T., Einarsson, K., & Sjövall, J. (1981) *J. Lipid Res. 22*, 404–409.
Ames, B. N., & Dubin, D. T. (1960) *J. Biol. Chem. 235*, 769–775.
Bevington, P. R. (1969) *Data Reduction and Error Analysis for the Physical Sciences*, McGraw-Hill, New York.
Booker, M. L., Scott, T. E., & La Morte, W. W. (1990a) *Gastroenterology 97*, 1261–1267.
Booker, M. L., Scott, T. E., & La Morte, W. W. (1990b) *Lipids 25*, 27–32.

Cabral, D. J., & Small, D. M. (1989) in *Handbook of Physiology—The Gastrointestinal System III, Section 6* (Schultz, S. G., Forte, J. G., & Rauner, B. B., Eds.) pp 621–662, American Physiology Society, Waverly Press, Baltimore, MD.

Cantafora, A., Angelico, M., Di Biase, A., Pièche U., Bracci, F., Attili, A. F., & Capocaccia, L. (1981) *Lipids 16*, 589–592.

Carey, M. C. (1985) in *Sterols and Bile Acids* (Danielsson, H., & Sjovall, J. Eds.) pp 345–403, Elsevier, Amsterdam.

Cohen, D. E., & Carey, M. C. (1991) *J. Lipid Res. 32*, 1291–1302.

Donovan, J. M., & Carey, M. C. (1990) *Hepatology 12*, 94S–105S.

Fullington, D. A., Shoemaker, D. G., & Nichols, J. W. (1990) *Biochemistry 29*, 879–886.

Hay, D. W., Cahalane, M. J., Timofeyeva, N., & Carey, M. C. (1993) *J. Lipid Res. 34*, 759–768.

Helm, C. A., Israelachvilli, J. N., & McGuiggan, P. M. (1989) *Science 246*, 919–922.

Himmel, M. E., & Squire, P. G. (1981) *J. Chromatogr. 210*, 443–452.

Hjelm, R. P., Jr., Thiyagarajan, P., & Alkan-Onyuksel, H. (1992) *J. Phys. Chem. 96*, 8653–8661.

Kajiyama, G., Kubota, S., Sasaki, H., Kawamoto, T., & Miyoshi, A. (1980) *Hiroshima J. Med. Sci. 29*, 133–141.

Kumosinski, T. F., & Pessen, H. (1985) *Methods Enzymol. 117*, 154–182.

Marquardt, D. W. (1963) *J. Soc. Ind. Appl. Math. 11*, 431–441.

Mazer, N. A., Benedek, G. B., & Carey, M. C. (1980) *Biochemistry 19*, 601–615.

Menger, F. M., Lee, J.-J., Aikens, P., & Davis, S. (1989) *J. Colloid Interface Sci. 129*, 185–191.

Nichols, J. W. (1988) *Biochemistry 27*, 3925–3931.

Nichols, J. W., & Ozarowski, J. (1990) *Biochemistry 29*, 4600–4606.

Nozaki, Y., Schecter, N. M., Reynolds, J. A., & Tanford, C. (1976) *Biochemistry 15*, 3884–3890.

Salvioli, G., Romani, M., Loria, P., Carulli, N., & Prandelli, J. M. (1985) *J. Hepatol. 1*, 291–300.

Shoemaker, D. G., & Nichols, J. W. (1990) *Biochemistry 29*, 5837–5842.

Shoemaker, D. G., & Nichols, J. W. (1992) *Biochemistry 31*, 3414–3420.

Staggers, J., Hernell, O., Stafford, R. J., & Carey, M. C. (1990) *Biochemistry 29*, 2028–2040.

Struck, D. K., Hoekstra, D., & Pagano, R. E. (1981) *Biochemistry 20*, 4093–4099.

Tables of the Error Function and Its Derivative (1954), NBS Applied Mathematics Series 41, U.S. Government Printing Office, Washington, DC.

Tanford, E. (1980) *The Hydrophobic Effect: Formation of Micelles and Biological Membranes*, Wiley, New York.

Ulmius, J., Lindblom, G., Wennerstrom, H., Johansson, L. B.-A., Fontell, K., Söderman, O., & Arvidson, G. (1982) *Biochemistry 21*, 1553–1560.